A Dual Circularly Polarized Ultrawideband Rectenna with High Efficiency for Wireless Energy Harvesting

Jian Liu and Jun Yi Li

School of Integrated Circuits
Guangdong University of Technology, Guangzhou, 510006, China
xzliujian@gdut.edu.cn, 18374203633@163.com

Abstract – This paper presents an ultrawideband dual circularly polarized (CP) rectenna for wireless energy harvesting (WEH) applications. It is mainly composed of a dual CP antenna and an ultrawideband rectifier. The receiving antenna is fed by a coplanar waveguide (CPW) and it has two input ports. The proposed ultrawideband rectifier has a two-cascaded voltage doubler configuration. This configuration means the proposed rectifier's input impedance has less sensitivity to frequency variation. Thus, a wide bandwidth can be achieved. For validation, a prototype is designed, fabricated and measured. The measured results show that the axial ratio (AR) bandwidth of the proposed rectenna is from 1.35 to 3.10 GHz (for AR $<$3 dB). In this frequency range, the rectenna's power conversion efficiency (PCE) is higher than 55%. These results indicate that the proposed rectenna is highly efficient and suitable for wideband high-efficiency WEH systems.

Index Terms – Coplanar waveguide (CPW), dual circularly polarized antenna, ultra-wideband rectifier, wireless energy harvesting (WEH).

I. INTRODUCTION

In recent years, the wireless energy harvesting (WEH) technique has attracted more and more attention as this technology can be employed to extend the battery life of some low-power electronic devices, such as wireless sensor networks (WSN) [1], RFID systems [2], and implantable medical devices [3]. Rectenna is a key component of a WEH system. Its main function is to receive the radio frequency (RF) electromagnetic energy and convert it into direct current (DC) power [4].

One of the most important performance parameters of the rectenna is power conversion efficiency (PCE). In order to improve PCE, various technologies have been investigated [5]-[8]. One approach is to employ multiband or broadband rectenna to increase the received RF power [9]-[12]. The main goal of this approach is to expand the operating bandwidth of the rectenna to cover more communication bands. In [9], a dual-band (2.45 and 5.8 GHz) rectenna was proposed. Its peak PCEs are 63% at 2.45 GHz and 54.8% at 5.8 GHz, respectively. A broadband rectenna (from 1.8 to 2.5 GHz) [10] was presented and its peak PCE is higher than 55% in the range 1.8-2.5 GHz. However, its operating bandwidth is not wide enough for covering most communication systems.

Another approach to enhance rectenna's PCE is to make the rectenna not only work efficiently in a wide bandwidth but also receive arbitrary polarization electromagnetic waves. This is because circular polarization rectenna is capable of receiving more energy from the complex environment with multipath reflection and refraction. Nevertheless, it is challenging to design a wideband rectenna with circularly polarized characteristics. A novel wideband resistance compress-ion network (WRCN) is proposed [11] to improve the impedance matching performance between the rectifier and circularly polarized antenna, enabling the rectenna to attain high PCE over a wide frequency and input power ranges. However, the rectenna has a relatively complicated structure. Moreover, due to the opposite rotation directions of the electric field of LHCP and RHCP, polarization loss occurs when the polarization direction of the receiving antenna (e.g. LHCP) does not match that of the transmitted wave (e.g. RHCP), leading to partial signals being unable to be effectively received. Dual circularly polarized antennas are capable of receiving both LHCP and RHCP signals. In [13], a dual CP rectenna is presented. Its PCE is around 51% within the frequency range of 5.75 and 5.83 GHz when the input power is 0.5 dBm. The inherent challenges in designing a broadband dual CP rectenna are bandwidth expansion and efficiency improvement.

In this paper, we propose an ultrawideband dual circularly polarized rectenna (1.35-3.37 GHz) for ambient wireless energy harvesting systems. The main contribution of this work can be summarized as two aspects. On the one hand, we propose a novel broadband dual circular polarized antenna. It features compact dimension and simple structure. On the other hand, we propose

Submitted On: January 23, 2024
Accepted On: April 26, 2024

https://doi.org/10.13052/2024.ACES.J.390311

an ultra-wideband rectifier with a compact physical size. Finally, we combine the proposed antenna and rectifier to implement an UWB rectenna with the capability of receiving arbitrary polarized electro-magnetic waves. The receiving antenna is a chamfered square patch with double U-shape branches fed by two orthogonal coplanar waveguide (CPW) ports. These two ports are used for generating simultaneous right-hand CP (RHCP) and left-hand CP (LHCP). The rectifier has a compact size as its input impedance matching network is very simple. Furthermore, the input impedance of the rectifier has less sensitivity to the frequency. This characteristic is beneficial for designing a wideband rectifier. The experimental results have verified the proposed design methodology. Moreover, we provide a design guideline for the proposed ultrawideband rectenna, summarized below.

Step 1: Specification Definition. Define the operational requirements and specifications of the rectenna, including the frequency range, efficiency.

Step 2: Antenna Design. Determine the dimensions and shape of the monopole antenna based on the desired operating frequency and other specifications. Select an appropriate ground plane configuration, substrate and feeding network. Take out the simulation in CST Studio Suite to optimize the physical sizes of the monopole antenna. Then, get the optimized parameters and good performance parameter (such as impedance matching bandwidth, port isolation, and axial ratio).

Step 3: Rectifier Design. Choose appropriate Schottky diodes. Take out the source-pull simulation to determine the optimum load (RL) and input power (Pin). Design a two cascaded voltage doubler topology and wideband impedance matching network. Tuning the parameters of microstrip lines to obtain optimum performance.

Step 4: Measurement. Fabricate the prototype of the rectenna and establish a testing platform to evaluate its performance.

II. ULTRAWIDEBAND RECTENNA DESIGN

A. Antenna design and analysis

The proposed dual circular polarized ultra-wideband antenna and its optimized dimensions are shown in Fig. 1. This antenna occupies an area of 60 mm * 60 mm.

Figure 2 illustrates the evolution of antenna design improvement using three prototypes. The corresponding plots for return loss (S_{11}), port isolation (S_{12}), radiation efficiency and axial ratio (AR) are shown in Fig. 3. The radiator of Ant 1 is a compact chamfered square patch with two orthogonal microstrip feed lines. When port 2 is terminated with a matched load and port 1 is excited, Ant 1-3 exhibit good symmetry and reciprocity properties. When port 2 is excited, similar characteristics can

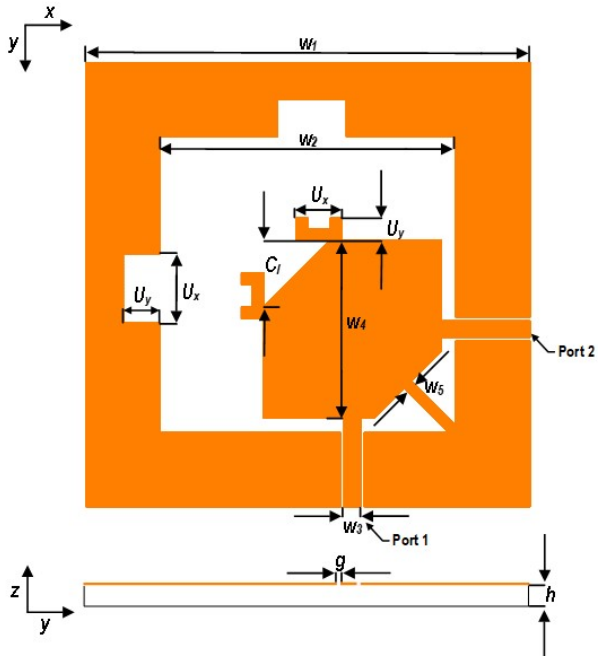

Fig. 1. Dual circular-polarized ultrawideband antenna with optimized dimensions (W1 = 60, W2 = 40, W3 = 2.2, W4 = 26, W5 = 1.3, h = 0.8, g = 0.5, Cl = 8.5, Ux = 9.4, Uy = 5, unit: millimeters).

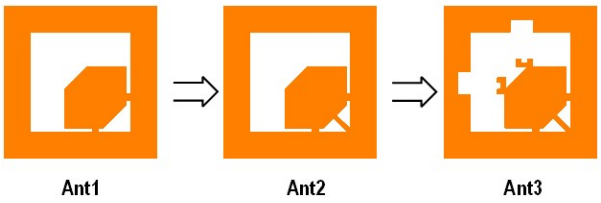

Fig. 2. Evolution of antenna.

be observed. From Figs. 2 and 3 (b) it can be observed that the two ports in Ant 1 are strongly coupled. Thus, we add a microstrip at the diagonal vertex of radiator to decouple the signals. Hence, within its operating frequency, Ant 2 provides 15-dB port isolation. Based on the above analysis, double U-shape branches are added in Ant 3 to modify the direction of electric currents, as shown in Fig. 4. Besides, two rectangular slots on the ground can be used to reduce the coupling between U-shape branches and the ground. The enhancement of AR bandwidth in comparison to that of Ant 2 is evident from Fig. 3 (c). According to Fig. 3 (d), it can be observed that Ant 3 achieves over 90% radiation efficiency within the 1.5-3.5 GHz frequency range. The surface current distributions of Ant 1-3 at 2.5 GHz are presented in Fig. 4. It can be observed that the currents are equal in amplitude and the flow direction is orthogonal at ωt = 0° and ωt

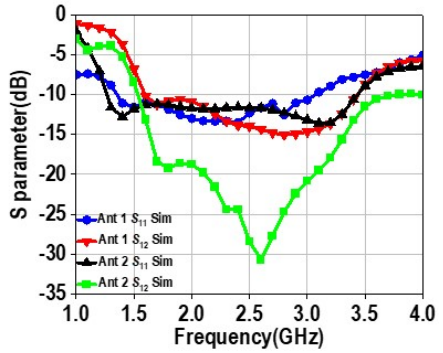

(a)

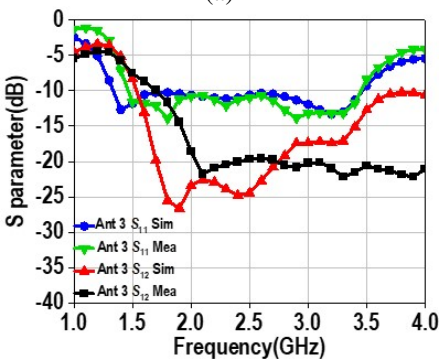

(b)

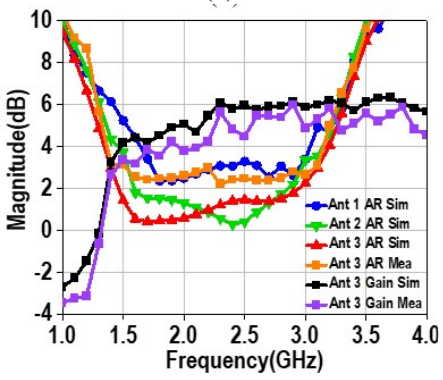

(c)

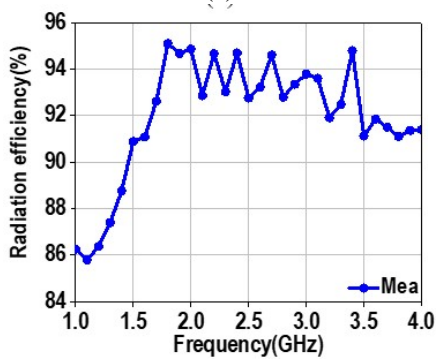

(d)

Fig. 3. Simulated and measured Ant 1-3: (a) return loss and port isolation of Ant 1-Ant 2, (b) return loss and port isolation of Ant 3, (c) gain and AR of Ant 1-Ant 3, and (d) radiation efficiency of Ant 3.

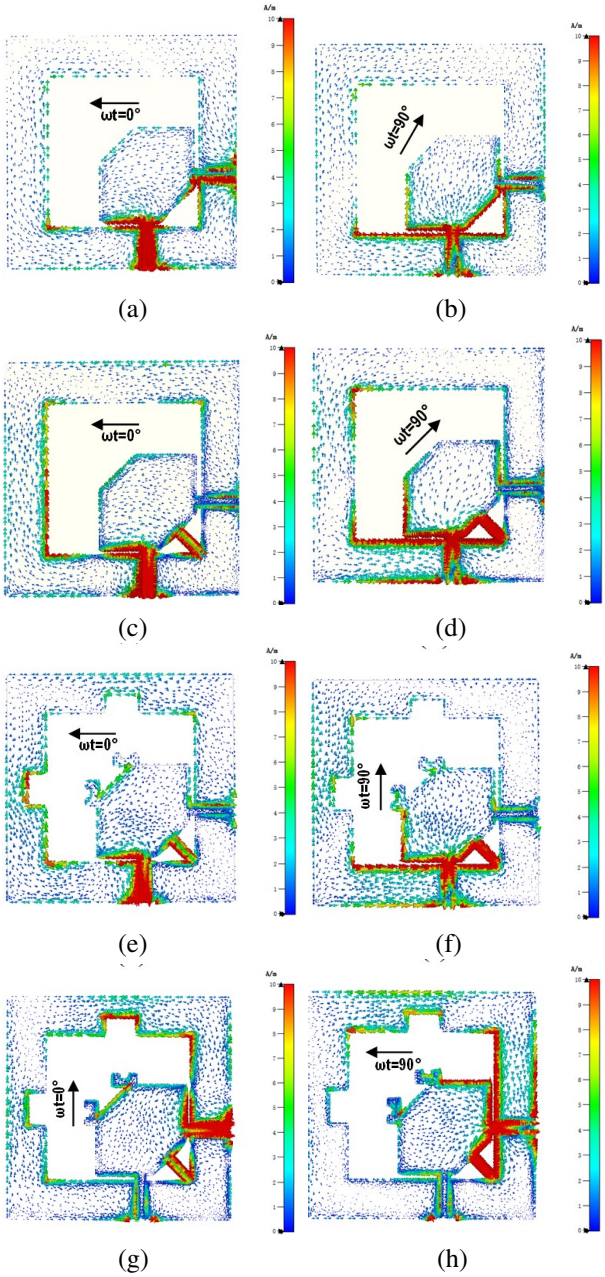

(a) (b) (c) (d) (e) (f) (g) (h)

Fig. 4. The surface current distributions at 2.5 GHz: (a) Ant 1 excitation at port 1, $\omega t = 0°$, (b) Ant 1 excitation at port 1, $\omega t = 90°$, (c) Ant 2 excitation at port 1, $\omega t = 0°$, (d) Ant 2 excitation at port 1, $\omega t = 90°$, (e) Ant 3 excitation at port 1, $\omega t = 0°$, (f) Ant 3 excitation at port 1, $\omega t = 90°$, (g) Ant 3 excitation at port 2, $\omega t = 0°$, and (h) Ant 3 excitation at port 2, $\omega t = 90°$.

$= 90°$. In this way, when port 1 is excited, the horizonal electric field component (E_h) leads the vertical electric field component (E_v) by approximately 90°. The rotation of current vector from $\omega t = 0°$ to $\omega t = 270°$ is clockwise. It illustrates that the antenna radiates LHCP waves

in the far field. when port 2 is excited, E_h lags E_v about 90°. The anticlockwise movement of the current vector shows the antenna radiates RHCP waves in the +z direction.

Figure 5 shows the normalized measured radiation patterns of Ant 3 in the *yoz* and *xoz* planes at 2.4 GHz and 2.5 GHz, which has a normalized pattern with a 10 dB radial scale. In the entire band, the RHCP fields radiated by the proposed antenna are stronger than the LHCP fields (cross-polarization) by more than 10 dB in the +z direction. Concurrently, the antenna emits LHCP fields with a 10 dB stronger intensity in the -z direction than the RHCP fields (cross-polarization). There is a good agreement between the simulation and measurement results. Based on the above discussion, it can be said that Ant 3 has ultrawideband and dual CP characteristics.

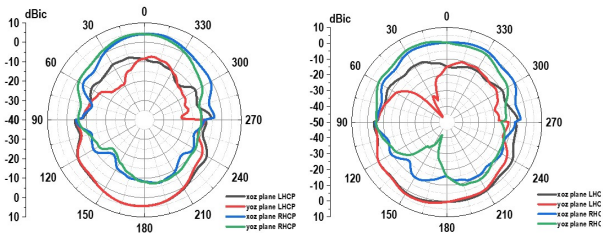

(a) (b)

Fig. 5. Measured normalized radiation patterns in the yoz and xoz planes at (a) 2.4 GHz and (b) 2.5 GHz.

B. Rectifier design and analysis

In this part, an ultrawideband rectifier is proposed. Figure 6 (a) shows the rectifier's schematic. As can be seen, this rectifier consists of a matching network, four Schottky diodes, dc-pass filter (C_4, C_5) and harmonic rejection filter (C_1, C_2, C_3). Figure 6 (b) gives the layout of the proposed rectifier. Table 1 lists the width and length of the microstrip lines. By using this novel topology structure, its impedance is less sensitive to frequency variation. This feature is beneficial for realizing a wideband rectifier. Thus, in this design, we use only a T-junction matching network to make the proposed rectifier achieve a wide impedance matching bandwidth.

To increase the conversion efficiency, it is necessary to suppress this energy [14]. The harmonic generation mechanism and higher order harmonic cancellation are

Table 1: Parameters of the microstrip lines

W_1	W_2	W_3	L_1 (L_{10})	L_2 (L_{11})	L_3 (L_{13})
2.2	0.9	0.8	1.9	2.1	3.3
L_4 (L_{14})	L_5	L_6	L_7 (L_{12})	L_8	L_9
3.3	3.4	1.9	2.3	2.4	2.4

(W: Width, L: Length, unit: millimeters).

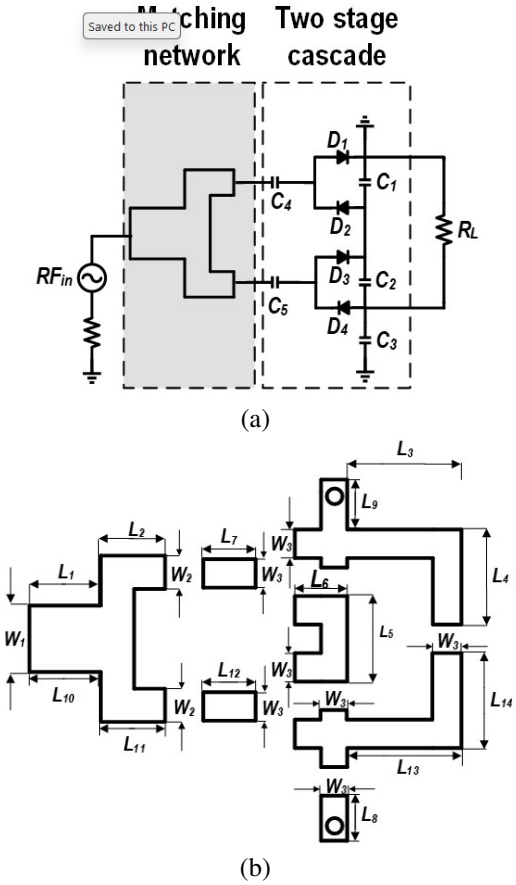

(a) (b)

Fig. 6. (a) Schematic and (b) layout of the proposed rectifier.

related. The two cascaded topology makes it easy to suppress the second order harmonics, and frequency multipliers commonly employ this technique to compress the second order harmonics [15]. It is noted that this topology rectifier also can be realized by using some other different Schottky diodes (for example, HSMS2862 and HSMS2852). To verify the above performance, the proposed rectifier is analyzed using harmonic balance simulation in Advance Design System (ADS) software.

The impedance of a single diode on shunt can be expressed as follows [16]:

$$Z_0 = \frac{\pi R_s}{\theta_{on} - \sin\theta_{on}\cos\theta_{on} + j\omega R_s C_j\left(\frac{\pi-\theta_{on}}{\cos\theta_{on}} + \sin\theta_{on}\right)}, \quad (1)$$

where C_j is the junction capacitance of diode, θ_{on} is the phase angle where the diode switches on, and R_s is the series resistance of diode. Figure 7 (a) displays input impedance of the proposed rectifier with HSMS2862 and HSMS2852. Here, the breakdown voltage of HSMS2862 is 7 V. When the frequency varies from 0.1 to 4 GHz, we can observe that the real part of the rectifier's input

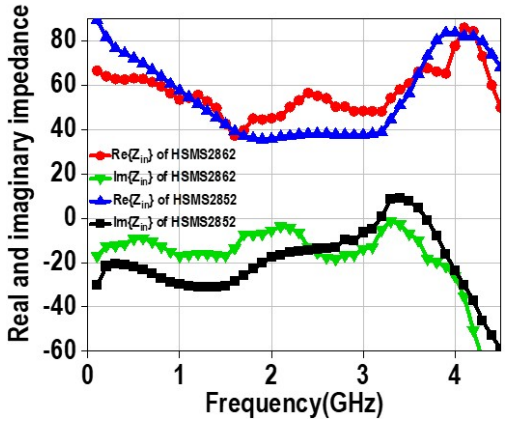

(a)

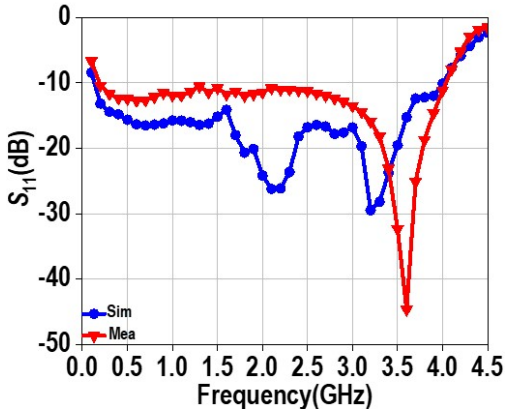

(b)

Fig. 7. The proposed rectifier (a) input impedance with HSMS2862, HSMS2852, and (b) simulated and measured S11 with HSMS2862.

impedance (Z_{in}) maintains around 50 Ohm (within the range of 40 and 65). In addition, the imaginary part of Z_{in} has a flat variation trend. Thus, we can say that the rectifier's input impedance is less sensitive to frequency variation. The simulated and measured reflection coefficients (S_{11}) with HSMS2862 are plotted in Fig. 7 (b). As can be seen, S_{11} is less than -10 dB when the frequency varies in the range of 0.1 and 4 GHz. The RF-DC power conversion efficiencies of the proposed rectifier with different diodes are plotted in Fig. 8. Different input power levels and load values are optimized for each diode. For HSMS2862 with 1200 Ohm load, the measured peak conversion efficiency is 73% at input power level of 18 dBm. Meanwhile, the conversion efficiency can remain over 60% within the impedance bandwidth. The simulated conversion effi-ciency for HSMS2852 over the frequency band (0.1-3 GHz) can be maintained above 40% with a 5 dBm input power level. Therefore, an ultrawideband rectifier can be designed by using this novel topology with different Schottky diodes.

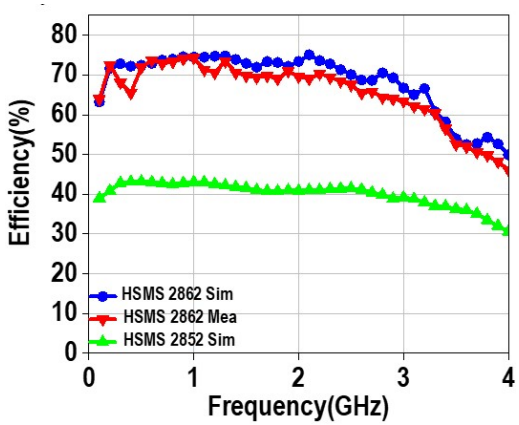

Fig. 8. Simulated and measured RF-DC PCEs versus frequency with different diodes.

III. RECTENNA IMPLEMENT AND MEASUREMENT

For validation, we designed and implemented an ultra-wideband rectenna, as shown in Fig. 9 (a). The antenna is fabricated on a 0.8 mm-thick FR4 substrate ($\varepsilon_r = 4.4$, $\tan\delta = 0.02$). A 0.762 mm thickness layer of Arlon AD255c ($\varepsilon_r = 2.55$, $\tan\delta = 0.0014$) is selected as the substrate for the rectifier. In order to make a trade-off between fabrication-cost and performance, the antenna and rectifier are fabricated by using two different substrates.

For the prototype, Murata capacitor (C_1, C_2, C_3) (330 pF), dc load (R_L) (1200 Ohm) and four diodes (HSMS2862) are used. Antenna and rectifier are connected by SMA connectors. The physical size of the antenna is 60 * 60 mm. The physical size of the proposed ultrawideband rectifier is 15 * 12 mm. The measurement system is shown in Fig. 9 (b).

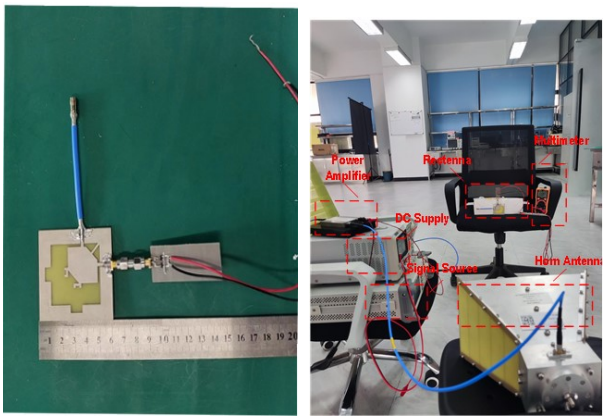

(a) (b)

Fig. 9. (a) Rectenna prototype and (b) measurement system.

Table 2: Comparison of the proposed rectenna and previous related design

Ref	Rectifier Topology	Diode Type	Frequency (**GHz**)	Polarization	Input Power (dBm)	Peak PCE(%)
[9]	Single series connection two stage	HSMS2860	2.4 and 5.8 (FBW: None)	LP	12	63% and 54.8%
[10]	voltage doubler	SMS7630	1.8 – 2.5 (FWB: 32.5%)	Dual LP	−35 to −10	70%
[11]	WRCN	HSMS2860	1.7 – 2.9 (FWB: 52.1%)	Dual CP	−3 to 20	76%
[12]	voltage doubler	HSMS2862	2.0 – 2.7 (FWB: 29.7%)	LP	18	72.5%
[13]	single series	HSMS2850	5.75 – 5.83 (FWB: 1.36%)	Dual CP, LP	0.5	51.1%
This work	two-stage voltage doubler	HSMS2862	1.35 – 3.37 (FWB : 85.5%)	Dual CP	18	67.3%

*FBW: Fractional bandwidth, LP: Linearly polarized, CP: Circularly polarized.

The RF signal source (RIGOL DSG3136B-IQ) generates the RF signal, which is subsequently amplified by the power amplifier (TLPA0.5G6G-35-30) and radiated by the horn antenna (HD-1018DRHA10S). The RF power is harvested and rectified by the horn antenna (HD-1018DRHA10S). The RF power is harvested and rectified by the proposed rectenna, then transmitted to the load. Finally, a multimeter is employed to measure the dc output voltage at the load terminal of the rectenna. Hence, the receiving power can be calculated as:

$$P_{in} = P_t G_t G_r \left(\frac{\lambda}{4\pi D}\right)^2, \tag{2}$$

where P_t is the energy from the signal generator, G_t is the horn antenna gain, G_r is the gain of the receiving antenna (5 dBi), and D (2.8 m) is the distance between the horn antenna and the rectenna.

The PCE of the rectenna is calculated below:

$$PCE = \frac{V_{out}^2}{R_L P_{in}} \times 100\% \tag{3}$$

where V_{out} is the measured output voltage on the R_L. Figure 10 shows the simulated and measured PCEs versus frequency with a 18 dBm input power. As seen, the proposed rectenna achieves a stable PCE. More specifically, its PCE is higher than 55% when the frequency varies within the range of 1 and 3.40 GHz. The measured peak PCE is 67.3% at 1.9 GHz. The measured PCEs versus input power at different frequencies are depicted in Fig. 11. There is a good agreement between the simulation and measurement results. A comparison of the proposed rectenna with some pervious work is presented in Table 2. It can be observed that the proposed rectenna not only achieves the widest fractional bandwidth (FBW) but also has dual CP characteristics.

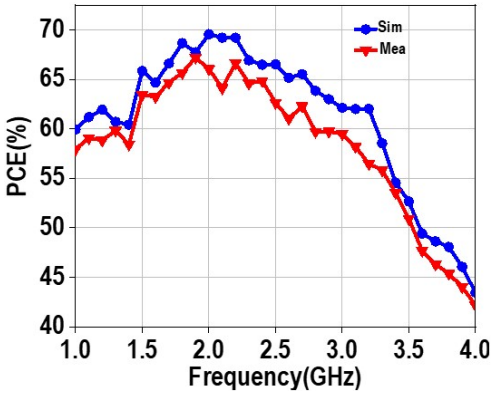

Fig. 10. Simulated and measured PCEs versus frequency at 18 dBm input power.

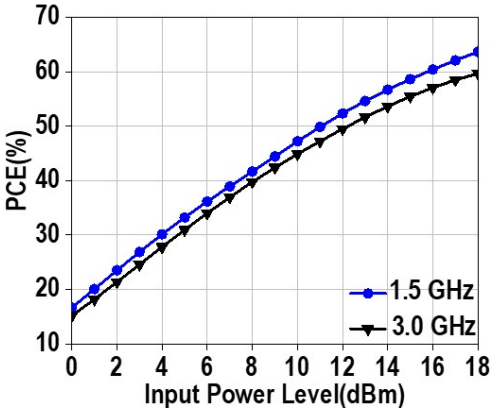

Fig. 11. The measured PCEs versus input power at 1.5 and 3.0 GHz.

IV. CONCLUSION

A compact dual circularly polarized ultrawideband rectenna is proposed for a WEH system. The experimental results demonstrate that the PCE of the proposed rectenna is higher than 55% from 1.35 GHz to 3.37 GHz, which covers multiple communication bands such as GSM-1800 (1.8 GHz), LTE 2.1 GHz, and WLAN (2.45 GHz). Furthermore, this compact rectenna exhibits the capability to receive incident electromagnetic waves with arbitrary polarization. Considering its excellent performance, it is anticipated that the proposed rectenna can be utilized in broadband WEH systems.

REFERENCES

[1] M. Kumar, S. Jain, and A. Sharma, "A plug-in type integrated rectenna cell for scalable RF battery using wireless energy harvesting system," *IEEE Microw. Wireless Compon. Lett.*, vol. 33, no. 1, pp. 98-101, June 2023.

[2] K. Niotaki, and N. B. Carvalho, "RF energy harvesting and wireless power transfer for energy autonomous wireless devices and RFIDs," *IEEE J. Microw.*, vol. 3, no. 2, pp. 763-782, Apr. 2023.

[3] L. Yang, Y. J. Zhou, C. Zhang, X. M. Yang, X. X. Yang, and C. Tan, "Compact multiband wireless energy harvesting based battery-free body area networks sensor for mobile healthcare," *IEEE J. Electromagn. RF Microw. Med. Biol.*, vol. 2, no. 2, pp. 109-115, June 2018.

[4] L. Guo, X. Li, W. Yang, Y. Zhao, and K. Wu, "Designing and modeling of a dual-band rectenna with compact dielectric resonator antenna," *IEEE Antennas Wireless Propag. Lett.*, vol. 21, no. 5, pp. 1046-1050, May 2022.

[5] L. Guo, X. Gu, P. Chu, S. Hemour, and K. Wu, "Collaboratively harvesting ambient radiofrequency and thermal energy," *IEEE Trans. Ind. Electron.*, vol. 67, no. 5, pp. 3736-3746, May 2020.

[6] S. Shen, C. Y. Chiu, and R. D. Murch, "A dual-port triple-band L-probe microstrip patch rectenna for ambient RF energy harvesting," *IEEE Antennas Wireless Propag. Lett.*, vol. 16, pp. 3071-3074, 2017.

[7] Y. Hu, S. Sun, H. Xu, and H. Sun, "Grid-array rectenna with wide angle coverage for effectively harvesting RF energy of low power density," *IEEE Trans. Microw. Theory Techn.*, vol. 67, no. 1, pp. 402-413, Jan. 2019.

[8] Y. Wang and J. Zhang, "Efficiency enhanced seven-band omnidirectional rectenna for RF energy harvesting," *IEEE Trans. Antennas Propag.*, vol. 70, no. 9, pp. 8473-8484, Sep. 2022.

[9] K. Bhatt, S. Kumar, P. Kumar, and C. C. Tripathi, "Highly efficient 2.4 and 5.8 GHz dual-band rectenna for energy harvesting applications," *IEEE Antennas Wireless Propag. Lett.*, vol. 18, no. 12, pp. 2637-2641, Dec. 2019.

[10] C. Song, Y. Huang, J. Zhou, J. Zhang, S. Yuan, and P. Carter, "A high efficiency broadband rectenna for ambient wireless energy harvesting," *IEEE Trans. Antennas Propag.*, vol. 63, no. 8, pp. 3486-3495, May 2015.

[11] Z. X. Du, S. F. Bo, Y. F. Cao, J. H. Ou, and X. Y. Zhang, "Broadband circularly polarized rectenna with wide dynamic-power-range for efficient wireless power transfer," *IEEE Access*, vol. 8, pp. 80561-80571, 2020.

[12] M. J. Nie, X. X. Yang, G. N. Tan, and B. Han, "A compact 2.45-GHz broadband rectenna using grounded coplanar waveguide," *IEEE Antennas Wireless Propag. Lett.*, vol. 14, pp. 986-989, Dec. 2015.

[13] P. Lu, C. Song, and K. M. Huang, "A two-port multipolarization rectenna with orthogonal hybrid coupler for simultaneous wireless information and power transfer (SWIPT)," *IEEE Trans. Antennas Propag.*, vol. 68, no. 10, pp. 6893-6905, Oct. 2020.

[14] Y. J. Ren and K. Chang, "5.8-GHz circularly polarized dual-diode rectenna and rectenna array for microwave power transmission," *IEEE Trans. Microw. Theory Techn.*, vol. 54, no. 4, pp. 1495-1502, June 2006.

[15] D. Shim, C. Mao, S. Sankaran, and K. O. Kenneth, "150 GHz complementary anti-parallel diode frequency tripler in 130 nm CMOS," *IEEE Microw. Wireless Compon. Lett.*, vol. 21, no. 1, pp. 43-45, Jan. 2011.

[16] S. Y. Zheng, W. L. Liu, and Y. M. Pan, "Design of an ultra-wideband high efficiency rectifier for wireless power transmission and harvesting applications," *IEEE Trans. Ind. Electron.*, vol. 15, no. 6, pp. 3334-3342, June 2019.

Jian Liu was born in Henan, China.

He received the Ph.D. degree in electronic engineering from South China University of Technology, Guangzhou, China, in 2018. He is currently an associate professor with the school of integrated circuits, Guangdong University of Technology. His research interests include RF integrated circuits and wireless power transmission.

Jun Yi Li was born in Hunan, China. He received the B.S. degree in information engineering from Hebei University of Engineering, Handan, China, in 2021. He is currently pursuing the M.S. degree in Guangdong University of Technology. His main research interests include wireless power transmission and broadband antenna.